JOURNAL OF MATERIALS SCIENCE 35 (2000) 4431–4438

Forming discontinuous fiber arrays by fracture of lubricated carbon-filament tows

T. S. CREASY
Center for Composite Materials, VHE602 MC0241, University of Southern California, Los Angeles, CA 90089-0241, USA
E-mail: creasy@almaak.usc.edu

This paper presents the results of a set of continuous-filament-tow fracturing experiments designed to produce highly collimated discontinuous-fiber-arrays with well-dispersed fractures. Discontinuous-fiber-arrays have at least two uses: reinforcing a matrix phase at high volume fraction and, when impregnated with a fluid, performing as a microrheometer. The lubricating fluid used for these experiments is uncured TCR epoxy, which may be stored at room temperature for up to one year. Tows with gauge lengths of 287, 362 and 400 mm were fractured into discontinuous fibers arrays during extension at four percent strain/min. Weibull analysis showed singlet failures were responsible for the fracture process of the two largest gauge length samples and multiplet failures accounted for the bulk of fracture at the shortest gauge length. Normal distributions approximated the filament length distribution at all gauge lengths. The longest gauge sample had the best distribution of filament breaks and had an average fiber length of 207 mm and a standard deviation of 65 mm.

1. Introduction

DFAs have interesting properties for both scientific experiments and structural applications. Manufacturers create DFAs from continuous-filament tow that passes through a proprietary stretch breaking process, e.g. the Shappe and DuPont LDF^{TM} processes. DFAs have at least two uses: reinforcing a matrix phase at high volume fraction and, when impregnated with a fluid, performing as a microrheometer. In the first case, the DFA allows forming operations that stretch a reinforced sheet in the fiber direction. Yet, with its highly collimated filaments, a DFA system will have the same fiber volume fraction found in continuous fiber systems. Although the discontinuities reduce the strength of the material, there are circumstances where the lower performance is acceptable if automation reduces the production cost of a complex-shape laminate.

The second DFA application, microrheology, is the measure of dynamic fluid properties in layers that are under 1 μm thick. The typical matrix layer thickness in polymer composites that contain aligned carbon fibers measuring 5–7 microns in diameter is one micron or less. The fluid impregnation process makes thinner fluid layers possible. If a fracturing process produces a favorable mean fiber length and fiber length distribution, fractured tow may be employed as a microrheometer [1]. Drawing the DFA tow in the fiber direction converts the global applied tensile strain rate into a local shear-strain-rate between filaments. Selecting the type of fiber, e.g. glass or carbon, and its surface treatment would provide a tool for measuring effects of these parameters on the dynamic viscosity at the microscopic level.

This work was performed to meet the following objectives:

1. Determine the properties needed in a highly collimated discontinuous-fiber-array (DFA) to get the rheological performance desired.
2. Determine how the failure response of filaments and fiber bundles may be applied to create a model stretch-breaking process that generates DFAs.

2. Theory

The two topics considered in this section are the effects of filament length on DFA systems and the fracture behavior of filaments and tows. First, the effect of filament length on the tensile stress response is reviewed. This provides target values of filament length. In the second topic, a review of the interactive failure response of filaments shows that these interactions must be minimized in order to produce a good DFA tow.

2.1. Effect of filament length

Unlike continuous-fiber reinforcements, impregnated DFA systems can stretch in the fiber direction. The resistance to the stretching is the elongational viscosity, which in an unfilled fluid is a shear-free-flow condition [2]. Although the globally applied flow is shear-free, relative filament motion generates a local shear flow

between filaments. Standard practice requires calling this viscosity an apparent value since a local shear stress and a strain rate gradient are present. The filaments generate the local shear flow in the following manner. Under the velocity gradient in the fluid, the filaments move with the velocity of their centroids within that gradient [3–6]. Since the centroids are distributed, each filament moves with a velocity that varies from the velocity of its neighbors. Studies of the elongational viscosity of DFA agree that the major effect of the relative motion is an increase in the apparent elongation viscosity and that increase scales with the square of the filament aspect ratio [7, 8]. Filament aspect ratio equals L/D, which is the length of the filament, L, divided by its diameter, D. The effect of this local shear flow on the tensile stress appears in this relation [9]:

$$\sigma = \left[3(1-f) + \frac{f}{\ln k}\left(\frac{L}{D}\right)^2\right]\eta\dot{\varepsilon} \qquad (1)$$

where the tensile stress σ is equal to the sum of two terms multiplied by the product of the shear viscosity η and the applied tensile strain rate $\dot{\varepsilon}$. The left-hand term, $3(1-f)$, accounts for the tensile stress in the fluid. The right-hand term represents the local shear flow contribution of the fiber volume fraction, f, the packing density of the fibers, k, and the fiber aspect ratio. The square of the aspect ratio is called the "stress magnification factor", since it increases the tensile stress of the system. In DFA systems the aspect ratio can be immense. If the average filament length is 20 mm with a diameter of 0.007 mm, the resulting stress magnification factor is over eight million. Therefore, the local shear-strain-rate may dominate the tensile stress measured while extending these systems at high strain rate.

When used as a composite reinforcement, Equation 1 shows that stretching DFA sheets at low tensile stress requires short filaments that reduce L/D, a low viscosity matrix, or both. Otherwise the equipment needed to form large sheets of the material would have to match the load requirements needed to stamp aluminum sheets at room temperature [1]. However, DFAs used in rheology may have any useful filament length as long as it provides the necessary magnification of strain rate for a given experiment since a single tow of filaments is extended.

2.2. Bundle and filament interaction effects during fracture

Single filaments of carbon fiber fracture with a spread of strain that the Weibull distribution models well [10–14]. Various researchers have applied the results of single filament tests to models of bundle testing [12–14]. The two effects that determine the measured response in bundle testing are the load transfer rules and the filament interactions. The analysis of Coleman showed that bundles of Weibull fibers would fail as a group at the fracture stress of the weakest filament. Coleman's model used an infinite number of filaments within the bundle. As each fiber failed individually, he assumed that the load distributed evenly among the remaining members. These assumptions lead to over-prediction of the bundle strength of typical tow. The deterministic method proposed by Masson and Bourgain applies in the practical case of finite numbers of filaments [13]. The "weakest" link effect is present whenever the number of filaments climbs above as few as 100 members. These results indicate that creating a distributed set of independent filament breaks is difficult with a Weibull bundle, because the failures become concentrated at the lowest failure strain within the group.

In addition to the weakest link effect, filament interactions drive bundle failure toward low strains. These interactions occur when a failed filament transfers its load to nearest-neighbor filaments during the elastic recoil that follows the break. Both Cowking *et al.* [10] and Okoroafor and Hill [11] used acoustic emission to study the fracture of lubricated glass fiber bundles at low strain rates of 0.25 and 0.08 %/min, respectively. Cowking's quasi-static method reduced the strain on the bundle after each filament broke and accomplished single filament failures, or "singlet" failure, through the entire experiment. Okoroafor and Hill used constant crosshead speed to break glass and Kevlar bundles [11]. Fig. 1 shows their data for Kevlar 29. This figure illustrates the difference found in the ideal two-parameter Weibull model and an experiment performed at low and steady extension rate. The plot of survivability on the ln(−ln)/ln scale shows that the shape parameter varies during the course of the experiment. Initially the slope of the Weibull curve is slightly negative since filaments within the bundle are not all perfectly aligned and therefore strain unevenly. This misalignment reduces the initial bundle modulus and the modulus will increase with additional strain as more filaments load up. When the Weibull curve reaches a minimum and the slope becomes positive for the remainder of the experiment, Okoroafor and Hill find two connected regions of linearity. The first is the singlet region wherein the filaments fail independently. The second is a "multiplet" region, where multiplet refers to two or more simultaneous or near-simultaneous failures. This higher slope region of the curve results in a precipitous drop in load and survivability as the remaining filaments rapidly fail. In the data shown, about 80 percent of the filaments failed in the region of multiplet failures.

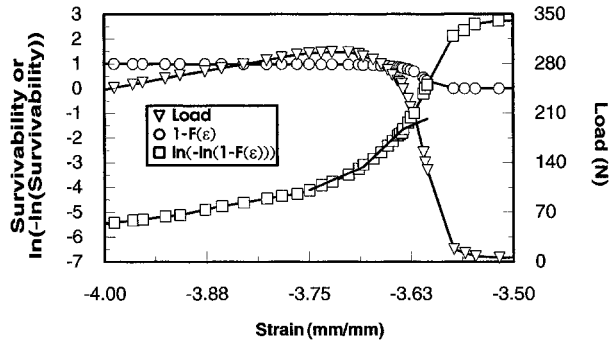

Figure 1 Kevlar 29 bundle fracture test from Okoroafor and Hill [11]. At high strain rate, the assumed singlet failure mode of the Weibull model gave way to multiple filament (multiplet) failures before complete bundle failure.

2.3. Proposed DFA process

The effects discussed above show that creating a DFA at high extension rates is challenging. A tow gripped in the traditional manner, e.g. highly aligned with a single filament length, fails over a more limited range of strain than found with single filaments. Therefore, the grip procedure used here–a helical wrap–attempts to create sub-groups of filaments that can fracture with greater independence from the whole bundle. The helical wrap end condition provides two effects that contribute to independent filament failure. One effect is a variation in the sample gauge length. The shorter gauge length section of the tow has a slightly higher strain rate than that applied to the longest section. As the tension continues, sub groups of filaments may fracture with filaments breaking at the stress of the subgroup's weakest member. This may distribute the failure of filament subgroups to a broader strain range. The second effect is a gradual reduction in the load within the tow from the straight section of the gauge length, which is fully loaded, to the clamped end of the wrapped filaments, which sees a load equal to the clamping force at most. Fig. 2 shows the three segments of the tow. A portion of the gauge length is straight and runs vertically between two rods. At each end of the straight section is a 250 mm length of tow for wrapping around the rods. For the breaking step, the inner 125 mm of this material wraps around the rods and clamps hold the tow to the rods. The final 125 mm of fiber at each end remains free and unloaded during the fracture process. Once the filaments are broken, the two sections of the bundle are separated by this procedure: the ends of the gauge section are unwrapped, the crosshead is moved to accommodate the extra 250 mm of straight tow, the unbroken 125 mm of the tow at the extremes are wrapped around the rods to provide the grip needed to extract the interleaved, discontinuous filaments through extension of the crosshead.

2.4. Extraction of Weibull parameters from bundle tests

Analyzing the failure of the filaments in this paper applied the method presented by Chi, Chou, and Shen [14]. They used the following equations to extract the Weibull shape and scale parameters from bundle test results. They calculate the survivability of the bundle:

$$1 - F(\varepsilon) = \exp\left[-L\left(\frac{\varepsilon}{\varepsilon_0}\right)^m\right] \tag{2}$$

Survivability equals one, less the strain to failure probability $F(\varepsilon)$ calculated from Weibull terms m, the shape parameter, and ε_0, the scale parameter, for filaments of length L at total strain ε. When survivability is plotted as $\ln(-\ln(1-F(\varepsilon)))$ versus $\ln\varepsilon$, the Weibull shape parameter m represents the slope of the curve. Using Equation 2, Chi, Chou, and Shen show that the load/strain curve for an ideal Weibull bundle comes from this relation:

$$P = AE_f\varepsilon N_0 \exp\left[-L\left(\frac{\varepsilon}{\varepsilon_0}\right)^m\right] \tag{3}$$

Fig. 3 displays the load and survivability data for an ideal filament bundle with values calculated for IM7 carbon fiber [14]. This ideal bundle has 12,000 filaments (N_0). The filament area (A) corresponds to a diameter of 5 μm. Filament modulus (E_f) is 169 GPa and length (L) is 100 mm. Weibull parameters used were typical of IM7 carbon fiber, that is, m of 7.78 and ε_0 of 0.028. Placing the load, survivability and Weibull data on one semi-log plot shows the change that occurs in each curve as the fracture process proceeds. The $\ln(-\ln)-\ln$ plot of the survivability data presents a straight line whose slope is the value of the Weibull shape parameter m; this paper refers to this plot as the Weibull curve and to the shape parameter as the Weibull slope. In the ideal case, the slope of the shape parameter curve is constant from the beginning of the experiment until the end. The modulus of the Weibull bundle decreases monotonically from its initial value as strain increases. Therefore, the two-parameter Weibull indicates that filament failure occurs from the very start of the loading process although, for uniformly aligned bundles, the failures should start at some minimum stress level that is much greater [12]. This is a good approximation for carefully controlled tests at low strain rates.

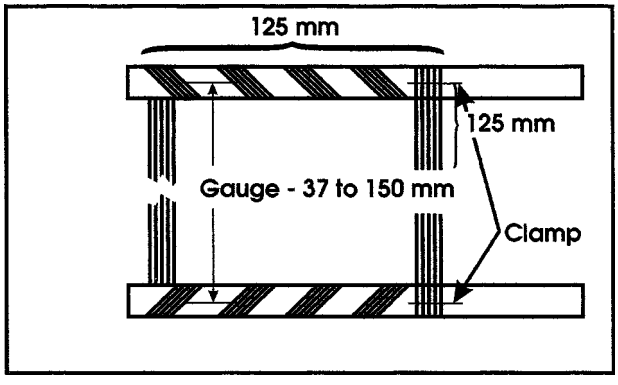

Figure 2 Diagram of the prepreg tow sample. This shows that the gauge length includes two regions of tow that wrap around the rods for 125 mm each. An additional 125 mm of fiber at each end provides the means of finding the endpoint of the breaking region and a means of gripping the fractured tow during the separation step.

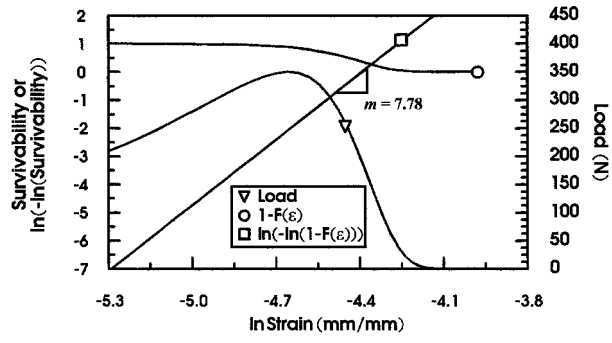

Figure 3 The ideal Weibull bundle of Chi, Chou and Shen under extension to total failure [14]. Bundle load peaks and then falls to zero as the filaments reach their maximum loads and fail. The survivability $(1-F(\varepsilon))$ of the filaments falls to zero (all fractured) as strain increases. The Weibull shape parameter, m, is constant throughout the process.

The plot of survivability in Fig. 3 shows that 99 percent of the filaments are intact when the load reaches 81 percent of the peak load. At the load peak, 88 percent of the filaments remain and failure with continued strain is gentle. Load and percent filaments remaining decrease at a moderate negative slope rather than as a sharp vertical drop.

3. Experimental

This section presents the details of the experiments including sample preparation, the method used to extend the tows until failure and the analysis of the length distribution obtained from the fracture process. These fracture experiments were a precursor to studying the rheological behavior of the impregnated DFA tows drawn under several strain rates. Those experiments used a design-of-experiments approach to quantify the effect of average filament length and extension velocity on the transient viscous or viscoelastic response of the bundle. That design selected three gauge lengths that ranged from the shortest to the longest possibly made with the fixtures used; therefore, carbon tows were broken at these gauge lengths: 287, 362, and 400 mm.

3.1. Sample preparation

The tow used in this study was a preimpregnated carbon fiber (IM7) that contained an uncured epoxy resin (TCR) as the matrix. The manufacturer stated that the fiber volume fraction for the spool was 56.1 percent. Spools contained approximately 450 g of the composite tow. Since twisting of the tow may change the fracture and extension response of the bundle, tow samples remained untwisted during these experiments.

An axle held the spool of prepreg tow above the workbench with the spool horizontal. A forceps clamped the free end of the tow and kept it from twisting as a sample was unrolled. Once enough material was unrolled, the another forceps clamped the tow so that the two could be used to fix the bundle to the test fixture. A straightedge razor blade cut the sample from the spool. Using the forceps, the tow was wrapped, without twisting, around the rods for 4.5 turns on each end. The number of turns came from a set of experiments that found three turns sufficient to hold the lubricated tow without slipping. The fourth wrap further reduced the load at the clamped end. The wrapping angle kept each turn of the tow from contacting the prior turn. Fig. 2 shows the various regions of a fiber sample. The 125 mm of tow wrapped around the rods have filaments breaking within them and they are part of the gauge length. The central section of the tow ran vertically between the rods and the length of this section was 37, 112, or 150 mm, depending upon the total gauge length desired.

3.2. Tensile extension

An Instron 8501P hydraulic-actuator tensile testmachine extended the tow. The machine pulled the impregnated tow to tensile failure of all of the filaments. While forming the DFA by the method presented below, rheological effects were avoided by using Equation 1 to set the tensile strain rate. The experiments performed for this paper create a DFA from an initially continuous tow. At the start of the test, the filaments stretch in parallel without relative motion to their neighbors; therefore, there are no local shear effects. As filaments fracture and the DFA forms, further extension of the tow generates a viscosity response since discontinuous filaments move relative to their neighbors. In the transition a mixed mode of tensile response exists with portions of the tensile load coming from the strain in the intact filaments and the balance coming from the viscous drag. At high strain rates, Equation 1 shows that the viscous component may contribute a substantial portion of the load. In order to analyze the breaking of the filaments, the strain rate must be low enough to keep the viscous contribution to a minor amount.

In this study, the apparent elongational viscosity of the DFA/TCR system at the longest mean filament length set the extension velocity used to fracture the carbon tow. Since the viscosity effect increases with the square of the aspect ratio, filaments broken with the longest gauge length have the largest viscous effect. Preliminary parametric experiments extended tow through the breaking process and continued at the same extension velocity into DFA stretching. At high strain rates, the elongation viscosity generated a tensile stress at a substantial fraction, i.e. greater than 50 percent, of the bundle breaking stress. At an extension rate of 12 mm/min the viscosity-induced load was less than five percent of the bundle fracture load. Therefore, this speed was used for the shorter gauge length samples as well.

3.3. Filament length measurement

The filament length distribution can be determined directly by manually separating filaments from the bundle and measuring their lengths. There are two problems with using this method. First, it is impractical to measure more than a small sample of the filaments. The small sample distribution must be converted into the actual distribution by statistical means, i.e., the method of likely extrema. Applying the statistical method requires assuming an appropriate distribution function for the filament length. Second, separating long individual carbon filaments from a tow produces questionable length distribution data since filaments can break during the process [13]. Therefore, the sampled distribution may have no relationship to the actual filament lengths within the tow. In this work the fractured tow's lineal mass distribution provided the length-distribution data shown in these results. Using mass distribution avoids the problems noted above since the entire tow provides the data. The lineal mass distribution of each half of the fractured tow describes the length distribution that it contains.

From the tow we must determine the filament length distribution, which is a probability density function $g(x)$, that is subject to these requirements:

$$P(a < l < b) = \int_a^b g(x)\,\mathrm{d}x$$
$$g(x) \geq 0 \quad \text{for all } x \tag{4}$$
$$\text{and} \int_{-\infty}^{\infty} g(x)\,\mathrm{d}x = 1$$

where l is a particular filament length, a and b describe a range of lengths, $g(x)$ is positive definite, and the total probability of finding filaments within the gauge length is 1. Integrating $g(x)$ twice obtains these relations:

$$G(x) = \int_{-\infty}^{x} g(t)\,\mathrm{d}t$$
$$\gamma(x) = \int_{-\infty}^{x} G(t)\,\mathrm{d}t \tag{5}$$

The functions $G(x)$ and $\gamma(x)$ are the cumulative distribution and its first integral, respectively. It is straightforward to show that $\gamma(x)$ is proportional to the lineal mass distribution collected in the following manner. After testing, half of the tow rested on a sheet of wax paper. With its overall lengths measured, it was sectioned into 12.7 mm pieces for weighing. As each piece joined the previous ones on the scale, the rising weight was recorded. Taking two derivatives of this mass data with respect to the tow length would produce the length distribution if the data were well behaved. However, this procedure is sensitive to the usual experimental variation in the mass measurement results and two derivatives of the data cannot be taken directly.

If a known statistical distribution fits the data, a suitable cumulative distribution [14] fit to the first derivative curve would allow a second derivative calculation. Rather than assume any specific distribution, several probability distributions were twice integrated to create a series of $\gamma(x)$ reference curves. The shape of the tow mass distribution compared to these curves indicates the most appropriate probability density function. A single derivative of the mass data is nondimensionalized and fit to the appropriate cumulative distribution function by a "least-squares" fit of the data.

Fig. 4 shows an example calculation of the length distribution for a 30 cm length of tow broken with a gauge length of 20 cm. The first data series in Fig. 4 is the distributed mass of the tow versus the sample length. The initial data lie outside of the gauge length, that is, the filaments are continuous. Here the lineal density (g/cm) is constant, which the constant slope indicates. Within the gauge length, the density falls as fewer and fewer filaments remain in the sample. Taking the first derivative of the mass data produces the lineal density shown by the second data series. Initially the density is constant; then it falls as the total number of filaments drops along the gauge length. A second derivative of the mass data generates the length-distribution curve with units of g/cm^2 shown in the final data series. Before the gauge section the distribution data are zero since there is no variation in length. The length varies across the gauge section and the curve describes that distribution.

When nondimensionalized, an appropriate statistical distribution fits the length-distribution curve in Fig. 4. In this example, a normal distribution from Choi [15] with the mean of $\mu = 10.0$ cm and the standard deviation $\psi = 3.1$ cm takes this form:

$$f(x) = \frac{1}{\sqrt{2\pi}\,\psi}\, e^{(-0.5)[(x-\mu)/\psi]^2} \tag{6}$$

The appropriate statistical distribution for a fractured tow is visible on a non-dimensional chart of mass versus length calculated from several standard distributions such as uniform or normal functions using multiple values of the standard deviation. Fig. 5 presents four curves calculated from twice-integrated statistical functions for one uniform and three normal distributions. The specific statistical functions integrated appear in Fig. 6. In Fig. 5 squares show the normalized

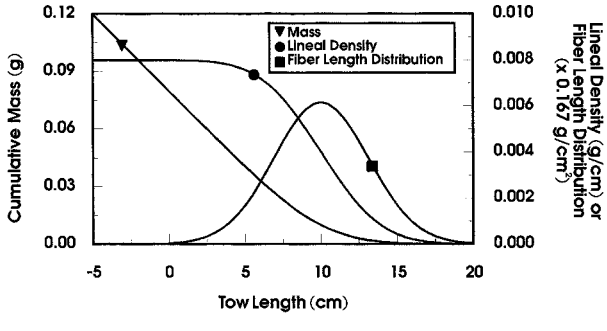

Figure 4 Linear mass distribution of a bundle of filaments calculated from a normal distribution of lengths with an average length of 10 cm and a standard deviation of ±3.12 cm. Twice integrating the length distribution obtains the cumulative mass shown as g versus cm.

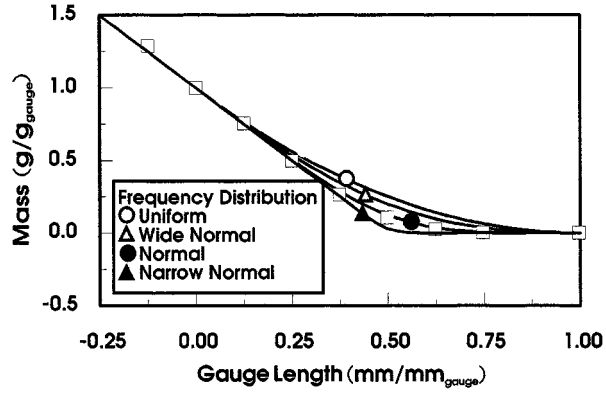

Figure 5 Mass data from fractured tow with 287 mm gauge length compared with the mass distribution derived from four statistical distributions: uniform, broad normal, normal, and narrow normal. Lines represent the calculation of the mass distribution from the twice-integrated statistical functions. Open squares show data from a 287 mm fractured tow. The normal distributions shown have a mean of one-half the gauge length and standard deviations of ±15, 31 and 100 percent of the mean. A normal distribution with a standard deviation of ±15 percent represented the mass distribution well.

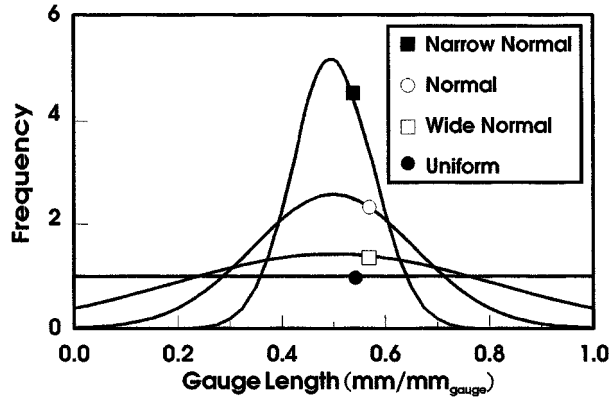

Figure 6 The uniform and normal statistical distributions integrated to obtain the theoretical tow mass distributions shown in Fig. 5.

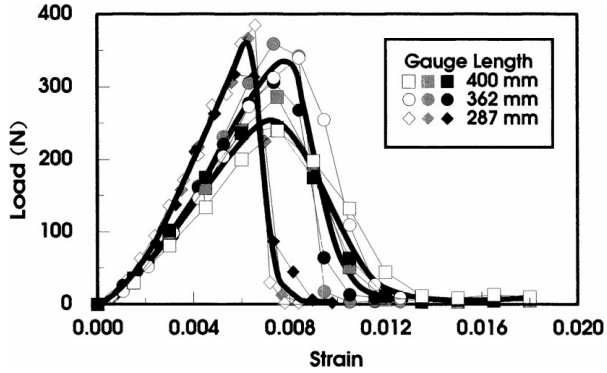

Figure 7 Collected fracture load-strain data for impregnated tow with gauge lengths of 287, 362 and 400 mm. The heavy lines are curves of the tests at each length that guide the eye and show the qualitative differences among the test samples.

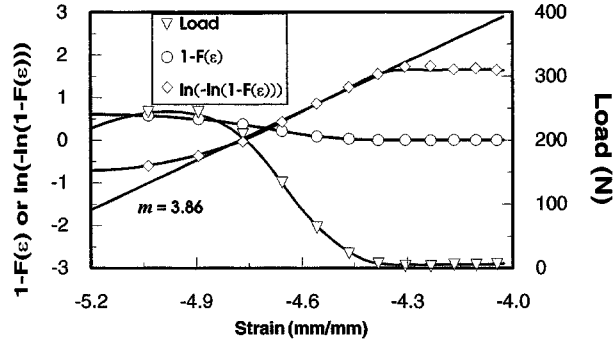

Figure 8 Bundle load, survivability, and Weibull slope for impregnated IM7 tow with a gauge length of 400 mm. The survivability starts at 61.8 percent indicating that 38.2 percent of the filaments failed before the bundle broke in the Weibull fashion. The shape parameter, m, rises to 3.8, which is lower than is typical of well aligned IM7 fiber.

mass distribution from one-half of a fractured carbon tow with a gauge length of 287 mm. The bundle is best represented by a normal distribution with a narrow standard deviation.

4. Results and discussion

The results appear here in the order obtained during the experiments. First, the fracture data show the effect of the helical end condition and rapid extension rate on the breaking stress for several gauge lengths. Finally, the length-distribution data show that this method effectively produces useful discontinuous samples.

A summary of the fracture data appears in Fig. 7 as load versus strain. There is an obvious difference in the tensile response of the 400 mm gauge length samples compared with the two shorter gauge lengths. The post-peak region of the 400 mm sample shows that the load falls in a gentle slope as opposed to the near vertical drop of the shorter samples. The shorter samples, gauge lengths 362 and 287 mm, show increasing similarity to traditional gripping techniques as the gauge length decreases. That is, the load rises with a greater slope and the post-peak load drop is nearly vertical. Samples at all gauge lengths show a modulus increase with strain as the shortest sub-bundles load up to failure and the load is taken up by an increasing percentage of the 12,000 filament tow. After reaching a maximum number of load-sharing filaments, the modulus falls again as filaments fail and the bundle separates.

4.1. Fracture and length distribution at 400 mm

Fig. 8 shows the bundle load, survivability, and Weibull plot data versus strain typical of the 400 mm gauge length samples. The survivability at the point of maximum bundle modulus indicates that only 62 percent of the filaments are intact at that point. This is well under the 99 percent expected for an ideal Coleman/Weibull bundle and the 80–90 percent found in typical bundles. Note that the remaining filaments cooperatively share the load and obtain a Weibull shape parameter value of 3.8 only after the peak load has passed. Therefore, 38 percent of the filaments failed in sub-bundle groups. This shape parameter is lower than the value of 7.78

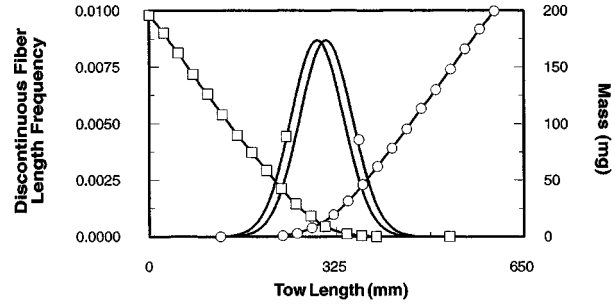

Figure 9 Mass and filament length distribution of a fractured tow with a gauge length of 400 mm. The lines are calculated from the normal distribution and the second integral of the distribution fit to each piece. Squares and circles represent the mass distribution data, except in the case of the frequency distribution where they indicate which distribution curve belongs to each section of the tow. The bottom and top sections have discontinuous filaments with average lengths of 229 and 184 mm, respectively. Standard deviation is broad, over ±40 mm, and the overall average filament length is 207 mm.

typical of IM7 filament bundles. This lower shape parameter and the gentle slope of the post-peak region imply that the filaments are failing independently and over a large range of strain. This result shows that well distributed filament breaks were achieved in the 400 mm gauge length as verified by the length distribution data that immediately follows.

Fig. 9 shows the mass distribution data and the resulting length distribution for the 400 mm gauge length. The square and circle symbols on the mass curves show the data points measured from the upper and lower sections of the tow. The lines connecting the points come from the second integral of the length frequency data shown in the figure. The two sections of the tow had average lengths of 229 and 184 mm. Their respective standard deviations were ±45 and ±42 mm. Interacting as an assembly of discontinuous filaments, the tow had an average length of 207 ± 45 mm, which is close to one-half the gauge length. The longest filament was 363 mm long; this is 91 percent of the gauge length. These results indicate that filaments broke within the helical section of the tow and almost to the position of the spring clamp. The wide spread of the filament lengths across the gauge shows that this tow is useful as a DFA for forming experiments. One factor that may have improved the response

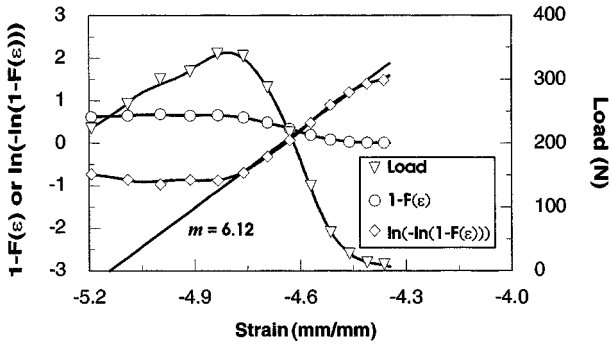

Figure 10 Bundle load, survivability, and Weibull slope for impregnated IM7 tow with a gauge length of 362 mm. The survivability starts at 68 percent when the bundle reaches maximum modulus. The shape parameter, *m*, rises to 7.8; this is typical of aligned IM7 fiber bundles.

of this long tow is the length effect of the filament flaws. With this long gauge-section and with the majority of the gauge section straight, the flaw population in the bundle is large and that may improve substantially the quality of the DFA. Indeed, as shown below, shortening the length of the bundle tended to concentrate the breaks.

4.2. Fracture and length distribution at 362 mm

The middle gauge length, 362 mm, produced the data shown in Fig. 10. The behavior is closer to the results of traditional bundle tests than that found at 400 mm. At maximum modulus 68 percent of filaments remain, a small increase from the prior result. The shape parameter reaches 7.8, which agrees with the published values for IM7 fiber. Note that the Weibull slope establishes this value just at the peak in the load.

Fig. 11 shows that this 9.5 percent shorter gauge length resulted in a 10 percent reduction in the average filament length of each tow section and the interactive average filament length. These values are 203 mm, 168 mm and 185.5 mm for the top, bottom and interactive averages respectively. Since the length distributions remain broad and the Weibull shape parameter single-valued, this gauge length is acceptable for making DFAs for experimentation.

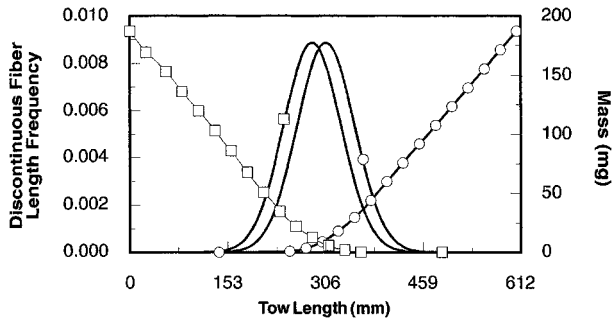

Figure 11 Mass and filament length distribution of fractured tows with a gauge length of 362 mm. Data for the top and bottom sections of a fractured tow are shown. The sections have discontinuous filaments with average lengths of 203 and 168 mm, respectively. Standard deviation is broad and the overall average filament length is 186 mm.

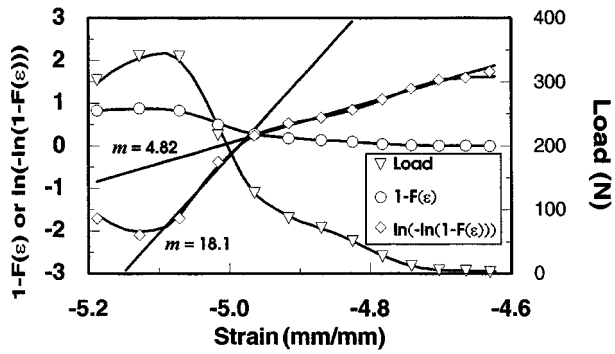

Figure 12 Bundle load, survivability, and Weibull slope for impregnated IM7 tow with a gauge length of 287 mm. The survivability starts at 88 percent when the bundle reaches maximum modulus; this is typical of aligned IM7 fiber bundles. The shape parameter, *m*, rises to 20.0, then falls to 5.0 at the end of the experiment. Multiplet fiber failure occurs during the early fracture of the bundle and then the final filaments fail individually.

4.3. Fracture and length distribution at 287 mm

Results for the shortest possible gauge length, 287 mm, indicate that there is a length effect in the fracture process. Fig. 12 shows that 88 percent of the filaments are intact at maximum modulus. This level of surviving fibers is closest to the usual bundle condition for tensile testing. However, the initial shape parameter is large at 20.0. Multiple simultaneous fiber breaks may be responsible for a Weibull slope of this magnitude [11]. After the initial fracture, when only 20 percent of the filaments remain, the shape parameter falls to 5.0; this indicates singlet failure among this last group of filaments. This result is the reverse of prior experiments at low strain rate [11]. There, the filaments transitioned from initial singlet failures to multiplet failures as strain increased. This concentration of failures is apparent in the mass and length distribution data.

Fig 13 shows that the length distribution in the tow is narrow. Average length for each piece is 57 and 51 mm for the top and bottom pieces of tow. Note that the mean lengths here are only 18.8 percent of the gauge length. This shows that the fiber breaks concentrated and did not use the entire span of the gauge length. The DFAs formed at the longer gauge lengths had mean lengths of 51.2 and 51.8 percent of the gauge length, which is near the ideal condition. Although shorter filament lengths

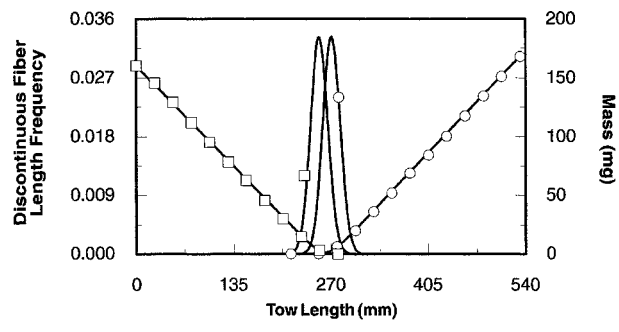

Figure 13 Mass and filament length distribution of fractured tows with a gauge length of 287 mm. The sections have discontinuous filaments with average lengths of 57 and 51 mm, respectively. Standard deviation is narrow and the average length is only 18.8 percent of the gauge length.

are desired, the strong effect of multiplet failures would make reproducible DFA forming difficult at this gauge.

5. Conclusions

With respect to the first objective of this work, it was determined that the shear strain magnification effect suggests that the filament length L should be as small as possible in order to avoid high tensile loads during drawing operations. This impacts the second objective, i.e., applying filament and bundle fracture behavior to a method of stretch breaking the fibers, since the process must make the shortest possible filaments with widely distributed breaks.

With regard to the second objective, the results show that forming well distributed DFAs is possible at high strain rate with large gauge length. The fully developed flaw density of the fiber keeps the failure loads low enough to avoid catastrophic failure. The filament lengths are long on average at 207 mm, but filament breaks were distributed well. At short gauge length, DFAs must be formed at low strain rates to avoid multiplet effects that turn the length distribution into a localized break. Since the highest filament strengths occur at short gauge-length the failure is catastrophic. Repeatability is difficult to achieve with a chaotic, interacting failure process.

As a reinforcing fiber, DFA may be formed at average filament lengths of 200 mm and strain rates of approximately four-percent strain/min. It may be possible to increase the strain rate until the average filament length begins to drop through interactions between fractured and intact filaments. However, strain rates must not be high enough to create viscous heating effects that could damage the resin.

As a microrheometer system, DFA can be produced in single tows of carbon fibers impregnated with the fluid of interest. Again, the tensile strain rate must be low enough to form the DFA structure without damaging the fluid, which is the sample of interest.

Finally, obtaining highly aligned filaments at significantly shorter lengths would require using a tow with a greater flaw density. Perhaps crimping the tow in a preliminary step could add enough flaws to reduce the filament length substantially.

Acknowledgements

The M. C. Gill Corporation supported this research through a postdoctoral fellowship at the University of Southern California. The Thiokol Corporation donated preimpregnated tow for the experiments.

References

1. T. S. CREASY, S. G. ADVANI and R. K. OKINE, *Journal of Rheology* **40** (1996) 497.
2. R. B. BIRD, R. C. ARMSTRONG and O. HASSAGER, "Dynamics of Polymeric Liquids, Volume 1" (John Wiley & Sons, New York, 1987) p. 104.
3. G. K. BATCHELOR, *Journal of Fluid Mechanics* **46** (1971) 813.
4. J. D. GODDARD, *ibid.* **78** (1976) 177.
5. *Idem., Journal of Non-Newtonian Fluid Mechanics* **1** (1976) 1.
6. A. J. BEAUSSART, J. W. S. HEARLE and R. B. PIPES, *Composites Science and Technology* **49** (1993) 335.
7. D. W. COFFIN and R. B. PIPES, *Composites Manufacturing* **2** (1991) 141.
8. S. M. DAVIS and K. P. MCALEA, *Polymer Composites* **11** (1990) 368.
9. T. S. CREASY and S. G. ADVANI, *Journal of Non-Newtonian Fluid Mechanics* **73** (1997) 261.
10. A. COWKING, A. ATTOU, A. M. SIDDIQUI, M. A. S. SWEET and R. HILL, *Journal of Materials Science* **26** (1991) 1301.
11. E. U. OKOROAFOR and R. HILL, *ibid.* **30** (1995) 4233.
12. B. D. COLEMAN, *Journal of the Mechanics and Physics of Solids* **7** (1958) 60.
13. J. J. MASSON and E. BOURGAIN, *Journal of Materials Science* **27** (1992) 3527.
14. Z. CHI, T. W. CHOU and G. SHEN, *ibid.* **19** (1984) 3319.
15. S. C. CHOI, "Introductory Applied Statistics in Science" (Prentice-Hall, Inc., Englewood Cliffs, New Jersey, 1978) p. 39

Received 8 December 1998
and accepted 8 February 2000